The Journal of Physiology

TRPM7 kinase activity regulates murine mast cell degranulation

Susanna Zierler[1,2], Adriana Sumoza-Toledo[1,4], Sayuri Suzuki[1], Fionán Ó Dúill[2], Lillia V. Ryazanova[3], Reinhold Penner[1], Alexey G. Ryazanov[3] and Andrea Fleig[1]

[1] *Center for Biomedical Research, The Queen's Medical Center and University of Hawaii John A. Burns School of Medicine and Cancer Center, Honolulu, HI 96813, USA*
[2] *Walther Straub Institute of Pharmacology and Toxicology, Ludwig-Maximilians-Universität München, 80336 Munich, Germany*
[3] *Department of Pharmacology, University of Medicine and Dentistry of New Jersey, Robert Wood Johnson Medical School, Piscataway, NJ 08854, USA*
[4] *Instituto de Investigaciones Médico-Biológicas, Universidad Veracruzana, Colonia Centro CP 91700, Veracruz, Mexico*

Key points

- The Mg^{2+} and Ca^{2+} conducting transient receptor potential melastatin 7 (TRPM7) channel–enzyme (chanzyme) has been implicated in immune cell function.
- Mice heterozygous for a TRPM7 kinase deletion are hyperallergic, while mice with a single point mutation at amino acid 1648, silencing kinase activity, are not.
- As mast cell mediators trigger allergic reactions, we here determine the function of TRPM7 in mast cell degranulation and histamine release.
- Our data establish that TRPM7 kinase activity regulates mast cell degranulation and release of histamine independently of TRPM7 channel function.
- Our findings suggest a regulatory role of TRPM7 kinase activity on intracellular Ca^{2+} and extracellular Mg^{2+} sensitivity of mast cell degranulation.

Abstract Transient receptor potential melastatin 7 (TRPM7) is a divalent ion channel with a C-terminally located α-kinase. Mice heterozygous for a TRPM7 kinase deletion ($TRPM7^{+/\Delta K}$) are hypomagnesaemic and hyperallergic. In contrast, mice carrying a single point mutation at amino acid 1648, which silences TRPM7 kinase activity ($TRPM7^{KR}$), are not hyperallergic and are resistant to systemic magnesium (Mg^{2+}) deprivation. Since allergic reactions are triggered by mast cell-mediated histamine release, we investigated the function of TRPM7 on mast cell degranulation and histamine release using wild-type ($TRPM7^{+/+}$), $TRPM7^{+/\Delta K}$ and $TRPM7^{KR}$ mice. We found that degranulation and histamine release proceeded independently of TRPM7 channel function. Furthermore, extracellular Mg^{2+} assured unperturbed IgE-DNP-dependent exocytosis, independently of TRPM7. However, impairment of TRPM7 kinase function suppressed IgE-DNP-dependent exocytosis, slowed the cellular degranulation rate, and diminished the sensitivity to intracellular calcium (Ca^{2+}) in G protein-induced exocytosis. In addition, G protein-coupled receptor (GPCR) stimulation revealed strong suppression of histamine release, whereas removal of extracellular Mg^{2+} caused the phenotype to revert. We conclude that the TRPM7 kinase activity regulates murine mast cell degranulation by changing its sensitivity to intracellular Ca^{2+} and affecting granular mobility and/or histamine contents.

(Received 9 September 2015; accepted after revision 10 December 2015; first published online 14 December 2015)
Corresponding authors A. Fleig: 1301 Punchbowl Street, Honolulu, HI 96813, USA. Email: afleig@hawaii.edu
S. Zierler: Goethestrasse 33, 80336 Munich, Germany. Email: susanna.zierler@lrz.uni-muenchen.de

Abbreviations CHS, contact hypersensitivity; GPCR, G protein-coupled receptor; SCG, superior cervical ganglion; TRPM7, transient receptor potential melastatin 7.

DOI: 10.1113/JP271564

Introduction

Magnesium (Mg^{2+}) is a required cofactor of many fundamental cellular reactions, including enzymatic reactions and G protein-mediated signalling (Killilea & Maier, 2008; Wolf & Trapani, 2008). Mg^{2+} also seems to play a role in immunological functions such as granulocyte oxidative burst, lymphocyte proliferation and endotoxin binding to monocytes (Johnson *et al.* 1980). Hypomagnesaemic rats show exacerbated inflammatory response to endotoxins (Malpuech-Brugere *et al.* 2000; Nakagawa *et al.* 2001), increased numbers of white blood cells (Mazur *et al.* 2007) and increased production of interleukin-1 (IL-1), tumour necrosis factor-α (TNF-α), interferon-γ (IFN-γ) and substance P (Weglicki & Phillips, 1992; Weglicki *et al.* 1992, 1994; Rude *et al.* 2005). In addition, Mg^{2+} deficiency in rats has been linked to increased plasma histamine levels originating from degranulation of mast cells (Kraeuter & Schwartz, 1980).

Cellular Mg^{2+} homeostasis is critically dependent on the ubiquitously expressed transient receptor potential melastatin 7 (TRPM7) ion channel (Nadler *et al.* 2001; Schmitz *et al.* 2003, 2004). TRPM7 is a bifunctional protein composed of a channel domain (TRPM7 channel) and an α-kinase domain (TRPM7 kinase) (Nadler *et al.* 2001; Runnels *et al.* 2001; Yamaguchi *et al.* 2001; Schmitz *et al.* 2003; Ryazanova *et al.* 2004). Annexin 1, myosin IIA and phospholipase Cγ2 are known *in vitro* substrates of the TRPM7 kinase (Dorovkov & Ryazanov, 2004; Clark *et al.* 2008; Deason-Towne *et al.* 2012). Regulation of gene transcription via histone modifications has also been attributed to TRPM7 kinase (Krapivinsky *et al.* 2014). The homeostatic TRPM7 ion channel is negatively inhibited by the synergistic interactions of cytosolic Mg^{2+} and Mg-nucleotides (Nadler *et al.* 2001; Schmitz *et al.* 2003, 2004) and by polyamines (Kozak *et al.* 2005).

The TRPM7 channel–kinase plays a critical role in embryonic development. Mice homozygous for a knock-out of the TRPM7 kinase domain proceed through a full day of gastrulation before being arrested at embryonic day 7.5 (Ryazanova *et al.* 2010). Heterozygous kinase domain knock-out mice ($TRPM7^{+/\Delta K}$) survive to adulthood, but manifest lower Mg^{2+} bone storage and Mg^{2+} urine levels when fed with a regular diet. When placed on low-Mg^{2+} diet, $TRPM7^{+/\Delta K}$ mice develop severe hypomagnesaemia leading to increased mortality and susceptibility to seizures and limb clasping compared to wild-type ($TRPM7^{+/+}$). In addition, $TRPM7^{+/\Delta K}$ mice manifest chemically induced allergic hypersensitivity on regular Mg^{2+} diet (Ryazanova *et al.* 2010), indicating modified immune responses. Interestingly, muting the kinase activity (Schmitz *et al.* 2003; Matsushita *et al.* 2005) by introducing a strategic point mutation in the ATP-binding domain ($TRPM7^{KR}$) does not replicate the phenotype of $TRPM7^{+/\Delta K}$ mice, but rather leaves mice insensitive to hypomagnesaemic conditions (Ryazanova *et al.* 2014).

Mast cells have long been considered as key effector cells in allergic inflammation. Mast cell degranulation in physiological conditions can be classified into two different types. One mainly depends on the increase of intracellular calcium concentration ($[Ca^{2+}]_i$) for the initiation of degranulation without involvement of trimeric G proteins (Gilfillan & Tkaczyk, 2006; Sagi-Eisenberg, 2007); the other is mediated by activation of trimeric G proteins, triggered by the stimulation of G protein-coupled receptors (GPCRs), such as chemokine receptors (Gilfillan & Tkaczyk, 2006; Kuehn & Gilfillan, 2007). These receptors are strongly dependent on intracellular Mg^{2+}, as receptor stimulation reduces the concentration of Mg^{2+} required for activation of G proteins by GTP (Birnbaumer & Birnbaumer, 1995). The chemokine macrophage inflammatory protein-1α (MIP-1α), for instance, is produced in mast cells following FcεRI aggregation. It is capable of inducing degranulation via the chemokine receptor CCR1, thus activating trimeric G proteins (Laffargue *et al.* 2002; Miyazaki *et al.* 2005). The neuropeptide substance P and other polycationic peptides stimulate mast cell degranulation receptor independently, via direct activation of G proteins (Lorenz *et al.* 1998).

Based on these observations, we examined the putative role of TRPM7 in degranulation and histamine release of peritoneal mast cells from $TRPM7^{+/+}$, $TRPM7^{+/\Delta K}$ and $TRPM7^{KR}$ mouse models. We found that G protein-induced mast cell degranulation and histamine release requires an operative TRPM7 kinase activity in primary murine mast cells.

Methods

Animals

The authors understand the ethical principles under which *The Journal of Physiology* operates and certify that their work complies with *The Journal*'s animal checklist (http://www.physoc.org/animal-experiments). The animal work was conducted under University of Hawaii Animal Care & Use Committee approved protocol no. 04-018-9, entitled 'TRPM Ion Channels in Pancreatic Beta and Immune Cells' in accordance with the US Animal Welfare Act and the National Research Council's *Guide for the Care and Use of Laboratory Animals*. All experiments involving animals at the LMU in Munich, Germany were performed in accordance with the EU Animal Welfare Act and were approved by the local councils on animal care (permit no. 55.2-1-54-2532-134-13 from District Government of Upper Bavaria, Germany). The use of transgenic animals was approved by the University of Hawaii Institutional Biosafety Committee protocol no. 15-08-213-02-3R, entitled 'TRPM Ion Channels in

Transgenic Mouse Tissue', and by the District Government of Upper Bavaria, protocol no. 821–8763.14.718/1210, respectively. Adult female and male wild-type and TRPM7 mutant *Mus musculus* ($TRPM7^{+/\Delta K}$ and $TRPM7^{KR}$) with a C57BL/6 background were bred and maintained at the University of Medicine and Dentistry of New Jersey, Robert Wood Johnson Medical School, as previously described (Ryazanova *et al.* 2010, 2014). Six- to eight-week-old mice were shipped to the University of Hawaii Animal and Veterinary Service Program and the animal facility of the Walther Straub Institute at the LMU Munich. Mice had unrestricted access to food and water. For mast cell isolation, mice were at least 8 weeks of age with a weight of at least 20 g. A total of 61 wild-type, 43 $TRPM7^{+/\Delta K}$ and 16$TRPM7^{KR}$ were killed. No animals were excluded, and there were no unexpected events.

Killing of mice

To isolate peritoneal mast cells, one mouse was killed to establish a primary cell culture that was viable between 1 and 2 days. The mouse was first anaesthetized by inhalation of 5% enflurane. After 2 min, anaesthesia was confirmed by gentle foot pinch reflex. The mouse was then killed by cervical dislocation while under anaesthesia. Tissue harvest followed as described (Penner *et al.* 1987).

Primary cell culture

Cells isolated from the peritoneum of $TRPM7^{+/+}$, $TRPM7^{+/\Delta K}$ or $TRPM7^{KR}$ mice were pelleted and apportioned (Cellgro, Mediatech, Manassas, VA, USA) into Petri dishes with poly-D-lysine-coated glass coverslips. Cells were cultured in 2 ml Dulbecco's modified Eagle's medium (DMEM) containing 10% fetal bovine serum (FBS) (HyClone, GE Healthcare) and 1 % penicillin–streptomycin (Gibco) overnight in a humidified incubator at 37°C and 5% CO_2. Mast cells were identified visually using light microscopy (phase contrast). For RT-PCR peritoneal mast cells were further sorted using an αCD117-FITC antibody (BioLegend, San Diego, CA, USA) and FACSAria III (BD Biosciences, Franklin Lakes, NJ, USA) at the Cell Sorting Core Facility, Institute for Cardiovascular Prevention, LMU München.

RT-PCR

Total RNA was extracted from fluorescence activated cell sorting (FACS)-sorted $CD117^+$ peritoneal mast cells as well as from kidney lysates using the GenElute mammalian total RNA purification kit (Sigma-Aldrich, St Louise, MO, USA). Prior to RNA extraction, shock frozen whole-kidney samples were lysed and homogenized in guanidine thiocyanate and 2-mercaptoethanol (GenElute, Sigma-Aldrich). First-strand cDNA synthesis was performed by the SuperScript® II reverse transcriptase (Invitrogen, Carlsbad, CA, USA). PCR was performed using REDTaq DNA polymerase (Sigma-Aldrich). To detect *Trpm6* transcripts we used primers Trpm6–forward 5′-CCAGCTCAAAAGACCCTCACAGATGC-3′ and Trpm6–reverse 5′-CACACCACATCTTTTCCGACCAG-3′ and the following PCR conditions: 94°C 3 min, 94°C 30 s, 56°C 30 s, 72°C 1 min, 35 cycles, 72°C 5 min. *Trpm7* transcripts were analysed using primers Trpm7–forward 5′-AGTAATTCAACCTGCCTCAA-3′ and Trpm7–reverse 5′- ATGGGTATCTCTTCTGTTATGTT-3′ with PCR settings: 94°C 5 min, 94°C 30 s, 50°C 30 s, 72°C 1 min, 35 cycles, 72°C 5 min. Amplified PCR products were 586 bp for *Trpm6* and 287 bp for *Trpm7*.

Electrophysiology

Patch-clamp experiments were performed using the whole-cell configuration. Currents were elicited by a ramp protocol from −100 mV to +100 mV over 50 ms, and acquired at 0.5 Hz and a holding potential of 0 mV. Inward current amplitudes were determined at –80 mV, outward currents at +80 mV and plotted *versus* time. Data were normalized to cell size as picoamps per picofarad. Capacitance was measured using the automated capacitance cancellation function of the EPC-9/10 (HEKA, Lambrecht, Germany). Values over time were normalized to the cell size measured immediately after whole-cell break-in. Average cell size at break-in for $TRPM7^{+/+}$ cells in physiological Mg^{2+} external solution was 7.05 ± 0.26 pF ($n = 46$) and in Mg^{2+}-free external solution 6.62 ± 0.22 pF ($n = 47$) ($P < 0.2$). For $TRPM7^{+/\Delta K}$ cells the average cell size at break-in in physiological Mg^{2+}-external solution was 7.51 ± 0.32 pF ($n = 64$) and in Mg^{2+}-free external solution 6.35 ± 0.30 pF ($n = 47$) ($P < 0.01$). For $TRPM7^{KR}$ cells average cell size at regular Mg^{2+}-external solution was 6.25 ± 0.29 pF ($n = 24$) and in Mg^{2+}-free external solution 6.88 ± 0.29 pF ($n = 36$) ($P < 0.08$). Standard extracellular solution contained (in mM): 140 NaCl, 1 $CaCl_2$, 2.8 KCl, 2 $MgCl_2$, 10 Hepes-NaOH, 11 glucose (pH 7.2, 300 mosmol l^{-1}). Nominally Mg^{2+}-free extracellular solution contained (in mM): 140 NaCl, 3 $CaCl_2$, 2.8 KCl, 0 $MgCl_2$, 10 Hepes-NaOH, 11 glucose (pH 7.2, 300 mosmol l^{-1}). Standard intracellular solution contained (in mM): 140 caesium glutamate (for acquiring TRPM7 currents) or 140 potassium glutamate (for degranulation experiments), 8 NaCl, 1 $MgCl_2$, 10 Hepes (pH 7.2, 300 mosmol l^{-1}). For $MgCl_2$ and $CaCl_2$ dose responses, intracellular solution contained (in mM): 120 potassium glutamate, 8 NaCl, 10 EGTA, and an appropriate amount of $MgCl_2$ or $CaCl_2$ was added, as calculated with WebMaxC.

Histamine assay

Cells were incubated in external solution containing 2 mM Mg^{2+} or without Mg^{2+} supplement for 1 h at 37°C and 5% CO_2. For IgE stimulation, cells were

pre-treated with 100 ng ml^{-1} IgE antibody against 2,4-dinitrophenylated (DNP)-bovine serum albumin (BSA) in DMEM overnight. The medium was exchanged and IgE Ab and 100 ng ml^{-1} DNP-BSA was added for another 30 min. Similarly, mast cells were treated with 100 ng ml^{-1} MIP-1α (30 min), 100 μM substance P (30 min). For inhibition of TRPM7 channel activity, cells were pre-incubated with 30 μM NS8593 (10 min), followed by simultaneous treatment with NS8593 and substance P (30 min). Homogeneous time-resolved fluorescence (HTRF®) was used to measure histamine release of differentially stimulated mast cells via a competitive immunoassay according to the manufacturer's instructions (Cisbio Bioassays, Parc Marcel Boiteux, Codolet, France; HTRF histamine assay cat. no. 62HTMPEB) (Claret *et al.* 2003). For sensitivity 100 readings were performed. Assay samples were prepared as triplets.

Immunofluorescence staining and confocal microscopy

Primary mouse peritoneal cells grown on glass coverslips were washed with Dulbecco's phosphate-buffered saline (DPBS) and fixed with 2% paraformaldehyde (PFA) (37°C) for 15 min at room temperature. Afterwards, cells were permeabilized with 0.2% Triton X-100 for 5 min at room temperature. Unspecific binding sites were blocked with 50 μl of FcR Blocking Reagent (Miltenyi Biotec GmbH, Bergisch Gladbach, Germany) (2.4:100) for 30 min at 37°C, followed by 2% BSA, 5% normal goat serum (NGS) in DPBS for 1 h at room temperature. Thereafter, cells were stained with a rat anti-TRPM7 antibody (kindly provided by T. Gudermann and V. Chubanov, Walther Straub Institute of Pharmacology and Toxicology, LMU Munich, Germany) (Chubanov *et al.* 2007), diluted 1:600 in blocking solution, for 1.5 h at 37ºC and a detecting antibody conjugated with Alexa 658 or Alexa 488 (goat anti-rat, Molecular Probes, 1:1200 in PBS) for 40 min at 37ºC. Cells were visualized via confocal microscopy (LSM510, Zeiss) using z-stack imaging and a plan-apochromat ×63/1.4 oil DIC objective with optical zoom of 3. Stacks ranged between 1.5 and 2 μm. The pinhole diameter was set to yield optical sections of 1.5 μm. For excitation, the 488 nm wavelength of an argon laser and 633 nm wavelengths of two helium–neon lasers were used. Emission was detected with band pass (BP) 505–530 nm and LP655 nm filters. Images were analysed using Zeiss LSM Image Browser (Carl Zeiss) and ImageJ (Research Services Branch, NIMH).

Rate analysis

For the capacitance fit, the following fit function was used:

$$f\,(\mathrm{x}) = c_{\mathrm{initial}} + (c_{\mathrm{initial}} \times (c_{\mathrm{max}} - 1) \times (1 - \exp(-\left(t_{\mathrm{delay}}\right)/\tau))^{n}),$$

where c_{initial} is the initial capacitance normalized to c_0, c_{max} is the degranulation amplitude normalized to c_0, c_0 is the capacitance at time point 0, t is the time in seconds. For the dose response fit we applied following formula:

$$f\,(\mathrm{x}) = (y_{\mathrm{min}} + (y_{\mathrm{max}} - y_{\mathrm{min}}) \times (1/(1 + (K_D/\mathrm{x})^{n}))),$$

with x representing the concentration, K_{D} the dissociation constant, and n the exponent.

Statistical analysis

Unless stated otherwise, data represent the mean of individual experiments ± standard error of mean (SEM). An unpaired Student's t test was applied for significance analysis and $P < 0.05$ was considered as statistically significant (*) and $P < 0.01$ as highly significant (**). Data represent the mean of individual cells ± SEM.

Results

Disruption of TRPM7 function perturbs G protein-induced mast cell degranulation

We have previously reported that heterozygous TRPM7$^{+/\Delta K}$ mice have significantly reduced TRPM7 channel activity, are hypomagnesaemic, and are more susceptible to allergic reactions (Ryazanova *et al.* 2010). We asked now whether the hyperallergic phenotype was due to a reduced availability of systemic magnesium (Mg^{2+}) or whether it was the result of dysfunctional mast cell degranulation caused by the disruption of TRPM7 function in the TRPM7$^{+/\Delta K}$ mice.

Allergic reactions are triggered by IgE-dependent mast cell degranulation (Ma & Beaven, 2009). We therefore investigated Ca^{2+}-induced degranulation in primary peritoneal mouse mast cells isolated from TRPM7$^{+/+}$ and TRPM7$^{+/\Delta K}$ mice. We measured fusion of mast cell granules to the plasma membrane using the whole-cell configuration of the patch-clamp technique, which allows assessing vesicle fusion-induced changes in capacitance of single cells via the automated capacitance compensation feature of the EPC amplifier (see Methods).

Peritoneal mast cells were perfused with internal standard potassium glutamate solution (see Methods). Cells were maintained in an external standard sodium-based solution containing 1 mM $CaCl_2$ and 2 mM $MgCl_2$. Internal calcium ($[Ca^{2+}]_i$) was clamped to a fixed value of 1 μM using an appropriate mixture of $CaCl_2$ and EGTA (see Methods). After whole-cell break-in, automatic capacitance compensation was performed at a frequency of 0.5 Hz. The initial value of cell capacitance obtained after break-in was used to normalize the experimental data to 1. Data were then averaged and plotted over the time of the experiment. We found that 1 μM $[Ca^{2+}]_i$ triggered exocytosis in both animal models to a similar

extent, reaching a plateau at 200 s with an ∼30% increase in cell size due to degranulation (Fig. 1*A* and *B*).

Mast cell degranulation can also be triggered by G protein activation (Penner & Neher, 1988; Pinxteren *et al.* 2000). In mice, G protein-induced mast cell degranulation is Ca^{2+} dependent (Aridor *et al.* 1993). Stimulation of G protein-mediated exocytosis by supplementing the internal solution with 100 μM GTPγS with $[Ca^{2+}]_i$ buffered to 600 nM enhanced mast cell degranulation in wild-type cells 5-fold compared to 1 μM $[Ca^{2+}]_i$ alone (Fig. 1*B* and *C*). However, degranulation in TRPM7$^{+/\Delta K}$ mast cells under these conditions was significantly suppressed compared to wild-type (Fig. 1*C*; $P < 0.025$). These data indicate that TRPM7 contributes to G protein-induced mast cell degranulation in mice.

Plasma membrane currents in wild-type and TRPM7 mutant peritoneal mast cells

The disruption of G protein-induced exocytosis observed in TRPM7$^{+/\Delta K}$ mice could be due to a reduction in TRPM7 expression, reduced TRPM7 channel activity, or impaired kinase function (Ryazanova *et al.* 2010). In addition, the mouse model is not homozygous for the kinase deletion, and thus some phosphotransferase activity might remain. To investigate this, we took advantage of an additional mouse model homozygous for a point mutation at amino acid position 1646, where lysine (K) is replaced with arginine (R) (TRPM7^{KR}). This mutation effectively inactivates the phosphotransferase activity of the TRPM7 kinase (Schmitz *et al.* 2003; Kaitsuka *et al.* 2014), while preserving the ion channel function, as assessed in embryonic fibroblasts (Ryazanova *et al.* 2014) as well as in peritoneal macrophages (Kaitsuka *et al.* 2014). Unlike mice homozygous for a complete removal of the kinase domain (TRPM7$^{\Delta K/\Delta K}$ mice), TRPM7^{KR} mice survive into adulthood (Kaitsuka *et al.* 2014; Ryazanova *et al.* 2014).

To measure the expression of TRPM7 and its closely related sister channel–enzyme, TRPM6, in purified murine mast cells we performed RT-PCR. Figure 2*A* demonstrates that TRPM7 is expressed in primary peritoneal mast cells, while TRPM6 transcripts are not detectable. On the other hand, both TRPM7 and TRPM6 transcripts are readily detectable in kidney lysates (Fig. 2*A*). Further, we labelled TRPM7 immunocytochemically (Chubanov *et al.* 2007) and analysed fluorescence signals in peritoneal mast cells using confocal microscopy. Figure 2*B* confirms the presence of TRPM7 protein in mast cells derived from TRPM7$^{+/+}$, TRPM7$^{+/\Delta K}$ and TRPM7^{KR}. Whole-cell patch-clamp studies corroborated this finding (Fig. 2*B* and *C*). Confirming our previous results and similarly to embryonic stem cells (Ryazanova *et al.* 2010), TRPM7 current amplitudes are reduced by half in TRPM7$^{+/\Delta K}$ mast cells (Fig. 2*C* left and middle panels). Just as in embryonic fibroblasts (Ryazanova *et al.* 2014) as well as in peritoneal macrophages (Kaitsuka *et al.* 2014), TRPM7 current activity in TRPM7^{KR} mast cells is identical to TRPM7$^{+/+}$ (Fig. 2*C* right panel). We also observed no differences in channel activation kinetics or current amplitudes when depleting intracellular Mg^{2+}

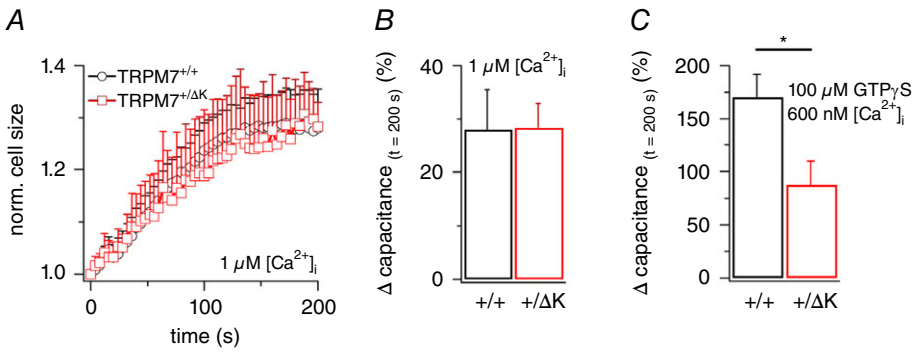

Figure 1. Suppression of G protein-induced degranulation in murine mast cells derived from heterozygous TRPM7$^{+/\Delta K}$ animals
A, average normalized capacitance measurements of Ca^{2+}-induced exocytosis (1 μM $[Ca^{2+}]_i$) in TRPM7$^{+/+}$ black circles) compared to TRPM7$^{+/\Delta K}$ (red squares) mast cells (n = 3–12). Capacitance as an estimate of cell size (in pF) was measured every 2 s using the capacitance cancellation function of the EPC9. The initial capacitance measured immediately after whole-cell break-in was used to normalize subsequent values, and was averaged and plotted *versus* time of the experiment. Intracellular Ca^{2+} concentration was clamped using the appropriate amount of EGTA and $CaCl_2$ (see Methods). *B*, percentage change in normalized degranulation amplitude of data in Fig 1*A*. Percentage change was assessed by subtracting the baseline of 1 from the data points at 200 s, and multiplying by 100 to achieve percentage values. Degranulation amplitude is plotted at 200 s into the experiment as percentage change in capacitance with error bars indicating SEM. *C*, percentage change in average degranulation amplitude of GTPγS-induced exocytosis (100 μM) and 600 nM $[Ca^{2+}]_i$ in TRPM7$^{+/+}$ (black bars) and TRPM7$^{+/\Delta K}$ (red bars) mast cells (n = 7–12) 200 s into the experiment. Statistical significance is indicated by the asterisk above the bars ($P < 0.025$).

and MgATP (Fig. 2*B* and *C*; Ryazanova *et al.* 2010). These data suggest that TRPM7 kinase activity does not affect TRPM7 channel function and kinetics in mast cells, similar to embryonic fibroblasts. Thus, $TRPM7^{KR}$-derived mast cells provide a unique cellular model to further study the mechanism on how TRPM7 is regulating G protein-induced murine mast cell degranulation.

TRPM7 kinase sensitizes G protein-triggered degranulation to $[Ca^{2+}]_i$

First, we established the $[Ca^{2+}]_i$ dependence of G protein-induced degranulation in all three mouse models by perfusing mast cells with 100 μM GTPγS under increasing $[Ca^{2+}]_i$ concentrations (Fig. 3). In $TRPM7^{+/+}$ mast cells, GTPγS induced exocytosis only above 300 nM $[Ca^{2+}]_i$, with an apparent EC_{50} for $[Ca^{2+}]_i$ of 400 nM and a steep Hill coefficient of 9, indicating an all-or-none response of degranulation under these conditions (Fig. 3*C*, open black circles).

Parallel experiments in $TRPM7^{+/\Delta K}$ and $TRPM7^{KR}$ mast cells revealed similar threshold levels for degranulation (Fig. 3*C*). However, G protein-induced mast cell degranulation at 600 nM $[Ca^{2+}]_i$ was strongly suppressed in both mouse models compared to wild-type: by 50% in $TRPM7^{+/\Delta K}$ mast cells ($P < 0.027$, Figs 1*C* and 3*A* and *C*) and by 60% in $TRPM7^{KR}$ mast cells ($P < 0.022$; Fig. 3*A* and *C*). Thus, G protein-mediated degranulation

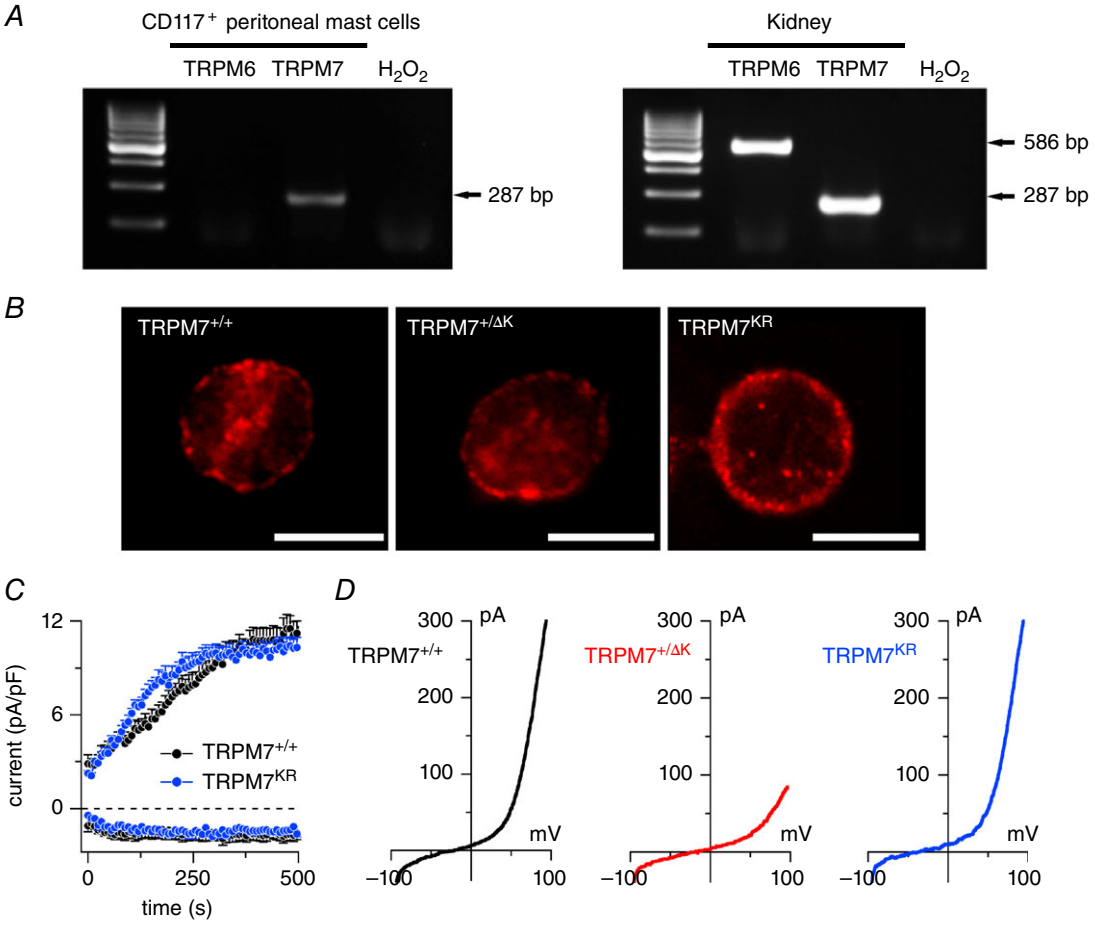

Figure 2. Expression and TRPM7 currents in wild-type and TRPM7 mutant peritoneal mast cells
A, RT-PCR analysis of TRPM6 and TRPM7 from FACS-sorted $CD117^+$ peritoneal mast cells (left) as well as from kidney lysates (right). A 100 kb ladder was used as a marker. Note that unlike in kidney controls, TRPM6 expression is absent in murine peritoneal mast cells. *B*, TRPM7 staining of $TRPM7^{+/+}$, $TRPM7^{+/\Delta K}$ and $TRPM7^{K1646R}$ ($TRPM7^{KR}$) mast cells. Scale bar indicates 5 μm. Note that TRPM7 expression pattern is similar in the three mouse phenotypes. *C*, TRPM7 current development in mast cells isolated from $TRPM7^{+/+}$ (black circles, $n = 8$) and $TRPM7^{KR}$ (blue circles, $n = 6$) mice. Cells were perfused with Mg^{2+}-free caesium glutamate internal solution (120 mM caesium glutamate, 5 mM EDTA plus 10 mM EGTA) to trigger optimal ion channel activation. Currents were elicited as described in Methods. *D*, current–voltage relationships (*I–V*) of representative mast cells for $TRPM7^{+/+}$ (black), $TRPM7^{+/\Delta K}$ (red) and $TRPM7^{KR}$ (blue) mutant extracted at 400 s. Note that in $TRPM7^{+/\Delta K}$-derived cells, TRPM7-like currents are strongly reduced as previously reported elsewhere (Ryazanova *et al.* 2010).

in the TRPM7 mutant mice has a more graded sensitivity to $[Ca^{2+}]_i$ changes compared to wild-type, effectively shifting both their EC_{50} by about 300 nM to the right (Fig. 3*C*). The analysis of the rate of release (see Methods for capacitance fit function) in all three mouse models revealed that a disruption of normal TRPM7 function not only desensitized G protein-induced degranulation to $[Ca^{2+}]_i$, but also slowed the rate of release compared to wild-type (Fig. 3*B*). This was most apparent in $TRPM7^{KR}$ mast cells, effectively slowing degranulation by more than 100% ($P < 0.056$). These findings indicate that the TRPM7 kinase activity is involved in G protein-induced degranulation by slowing the rate of degranulation and shifting its sensitivity to $[Ca^{2+}]_i$ within its physiological range in murine peritoneal mast cells.

TRPM7 kinase is essential for functional G protein coupled receptor-activated histamine release

Next, we asked whether the reduced sensitivity of G protein-induced mast cell degranulation, as seen in whole-cell experiments using the TRPM7 mouse mutants, would also have physiological consequences for histamine release. Mast cells will release histamine upon G protein-linked agonist stimulation through MIP-1α and substance P (Miyazaki *et al.* 2005; Bischoff, 2007). Thus, we induced histamine release in mast cells isolated from our three mouse models, $TRPM7^{+/+}$, $TRPM7^{+/\Delta K}$ and$TRPM7^{KR}$, with either 100 nM MIP-1α or 10 μM substance P using a homogeneous time-resolved fluorescence (HTRF) system. Histamine was measured by competitive enzyme-linked immunosorbent assay (ELISA) (Claret *et al.* 2003). Cells were incubated in 500 μl external solution supplemented with 2 mM Mg^{2+}. For quantification we normalized the measured histamine release to the spontaneous release of respective resting controls. Our results show that both mouse mutants $TRPM7^{+/\Delta K}$ and$TRPM7^{KR}$ had significantly suppressed histamine release compared to control when exposed to 100 nM MIP-1α (Fig. 4*A*; $P < 0.0065$ ($TRPM7^{+/+}$/$TRPM7^{+/\Delta K}$) and $P < 0.0033$ ($TRPM7^{+/+}$/$TRPM7^{KR}$)) or 10 μM substance P (Fig. 4*B*; $P < 0.003$ ($TRPM7^{+/+}$/$TRPM7^{+/\Delta K}$) and $P < 0.041$ ($TRPM7^{+/+}$/$TRPM7^{KR}$)).

Since $TRPM7^{KR}$ mice are not hypomagnesaemic, but $TRPM7^{+/\Delta K}$ mice are, we next investigated the role of extracellular Mg^{2+}. We repeated the MIP-1α and substance P experiments on mast cell activation and histamine release, but this time under nominally free external Mg^{2+} conditions. While the presence or absence of extracellular Mg^{2+} had no influence on histamine release in $TRPM7^{+/+}$ (see Fig. 4*A*, *B* and *C*, *D*), the absence of external Mg^{2+} completely eliminated the inhibitory effect on histamine release seen under normal conditions in both TRPM7 mutant mast cells. We observed strongly enhanced histamine release by about 2-fold when using MIP-1α stimulation (Fig. 4*C*, $P < 0.002$ and $P < 0.03$, respectively). Substance P also reversed the TRPM7 mutant phenotype, bringing histamine release back to slightly above wild-type levels in 0 mM Mg^{2+} conditions (Fig. 4*D*; $P < 0.005$ and $P < 0.014$, respectively). We conclude that a functionally disrupted TRPM7 activity sensitizes histamine release to extracellular Mg^{2+} status in peritoneal murine mast cells.

Finally, we tested whether blocking the channel pore of TRPM7 would alter substance P-induced histamine release in wild-type mast cells. Application of the TRPM7

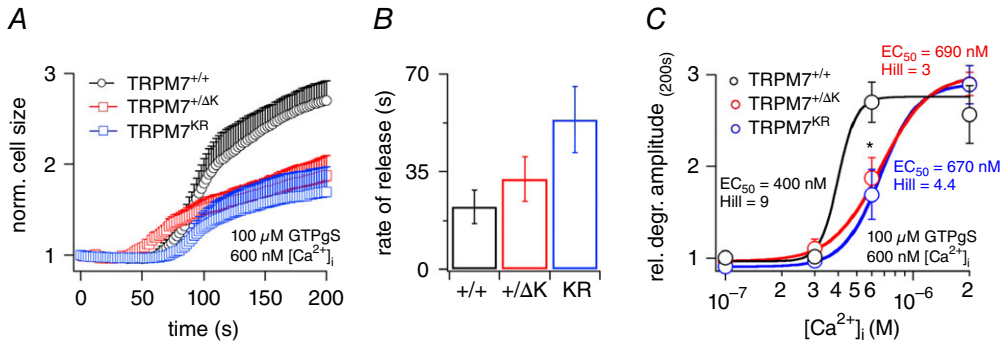

Figure 3. TRPM7 kinase regulates $[Ca^{2+}]_i$ sensitivity of G protein-triggered mast cell degranulation
A, capacitance measurements of 100 μM GTPγS-induced exocytosis in the presence of 600 nM clamped $[Ca^{2+}]_i$ in $TRPM7^{+/+}$ (open black circles, $n = 5$), $TRPM7^{+/\Delta K}$ (open red squares, $n = 5$) and $TRPM7^{KR}$ (open blue squares, $n = 6$) mast cells. The intracellular solution was buffered to 600 nM $[Ca^{2+}]_i$ using EGTA as chelator and appropriate amounts of $CaCl_2$. Data acquisition and analysis were as in Fig. 1*A*. *B*, analysis of the rate of release assessed from the data in *A*. $P < 0.056$ between $TRPM7^{+/+}$ and $TRPM7^{KR}$. *C*, intracellular Ca^{2+} dependency of G protein-mediated exocytosis (100 μM GTPγS) in $TRPM7^{+/+}$ (open black circles, $n = 5$–10), $TRPM7^{+/\Delta K}$ (red circles, $n = 5$–10) and $TRPM7^{KR}$ (blue circles, $n = 5$–7) mast cells. Same analysis as in *A*. EC_{50} and Hill coefficients as indicated in the panel. $[Ca^{2+}]_i$ was clamped using EGTA (10 mM). Asterisk indicates $P < 0.027$ for $TRPM7^{+/\Delta K}$ and $P < 0.022$ for $TRPM7^{KR}$. Error bars indicate SEM.

inhibitor NS8593 (30 μM) onto fully developed native TRPM7 currents in wild-type mast cells completely suppressed current activity (Fig. 4*E*), and this was independent of $[Mg^{2+}]_o$ (Fig. 4*F*) (Chubanov *et al.* 2012). In line with our previous results, no significant difference was found in substance P-induced histamine release when blocking TRPM7 channel activity with NS8593 (Fig. 4*G* and *H*). This provides further evidence that the TRPM7 ion channel function has no direct involvement in mast cell degranulation and that the observed effect is due to disrupted TRPM7 kinase activity.

Extracellular Mg^{2+} sensitizes Ca^{2+}-dependent mast cell degranulation

Our data show that a functionally impaired TRPM7 kinase sensitizes G protein-linked mast cell degranulation to hypomagnesaemic conditions. However, the data do not explain our *in vivo* results of the oxazolone allergy test, where the heterozygous $TRPM7^{+/\Delta K}$ mouse manifests a hyper-allergic phenotype, whereas the homozygous $TRPM7^{KR}$ mutant has hypo-allergic tendencies compared to wild-type (Ryazanova *et al.* 2010, 2014). Oxazolone is thought to mimic IgE-DNP-induced mast cell degranulation mediated through Ca^{2+} signalling (Kobayashi *et al.* 2010). We therefore turned our attention back to Ca^{2+}-induced mast cell degranulation.

Our initial data shown in Fig. 1 indicated that exocytosis at 1 μM $[Ca^{2+}]_i$ was identical between wild-type and $TRPM7^{+/\Delta K}$ mast cell degranulation under normal Mg^{2+} conditions (2 mM) (Fig. 1*A*). Furthermore, no difference was found between $TRPM7^{+/+}$ and $TRPM7^{+/\Delta K}$ in the graded dose–response behaviour of Ca^{2+}-dependent degranulation (Fig. 5*C* and *G*). Repeating

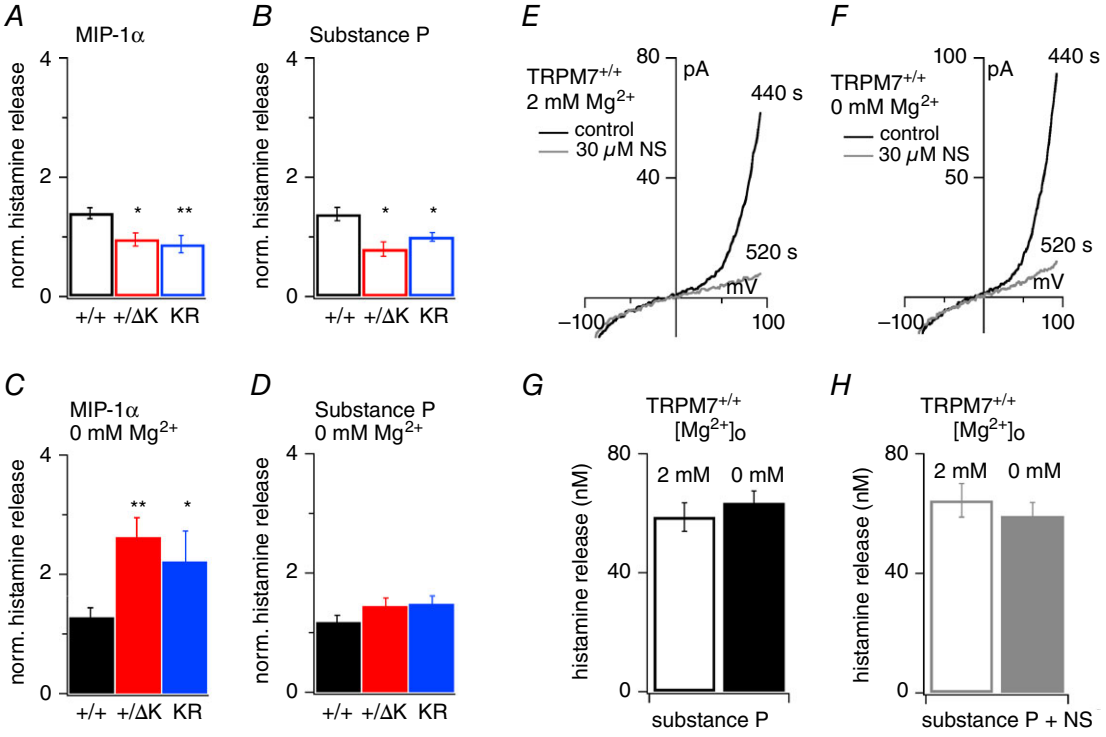

Figure 4. TRPM7 kinase is essential for G protein-coupled receptor-activated histamine release
A–D, histamine release of mast cells from $TRPM7^{+/+}$ (black), $TRPM7^{+/\Delta K}$ (red) and $TRPM7^{KR}$ (blue) mutant mice, normalized to spontaneous release rate at 30 min. Data represent means of at least 3 independent experiments ± SEM. *A*, peritoneal cells were stimulated with 100 nM MIP-1α in the presence of 2 mM Mg^{2+}. $TRPM7^{+/\Delta K}$ and $TRPM7^{KR}$ were strongly suppressed compared to control ($P < 0.033$ and 0.0065, respectively). *B*, peritoneal cells were stimulated with 10 μM substance P in the presence of 2 mM Mg^{2+}. Histamine release was strongly suppressed in $TRPM7^{+/\Delta K}$ and $TRPM7^{KR}$ compared to control; $P < 0034$ and 0.041, respectively. *C*, peritoneal cells were stimulated with 100 nM MIP-1α in the absence of Mg^{2+} (0 mM). $TRPM7^{+/\Delta K}$ and $TRPM7^{KR}$ histamine contents both exceeded wild-type by about 100% under these conditions ($P < 0.0019$ and 0.03, respectively). *D*, peritoneal cells were stimulated with 10 μM substance P in the absence of Mg^{2+}. *E* and *F*, representative *I–V* curves extracted from $TRPM7^{+/+}$ peritoneal mast cells perfused with Mg^{2+}-free internal solution (140 mM potassium glutamate, 10 mM EGTA) in the presence (2 mM Mg^{2+}, *A*; left) or absence of Mg^{2+} (0 mM Mg^{2+}, *B*; right), before (black trace) or during (grey trace) application of 30 μM NS8593, a the potent TRPM7 channel inhibitor. *G* and *H*, G protein-mediated histamine release (100 μM substance P) of $TRPM7^{+/+}$ mast cells with (open bars) and without (filled bars) the presence of external Mg^{2+}. Note that inhibition of channel activity using 30 μM NS8593 does not affect quantity nor Mg^{2+} sensitivity of histamine release (black *vs.* grey bars).

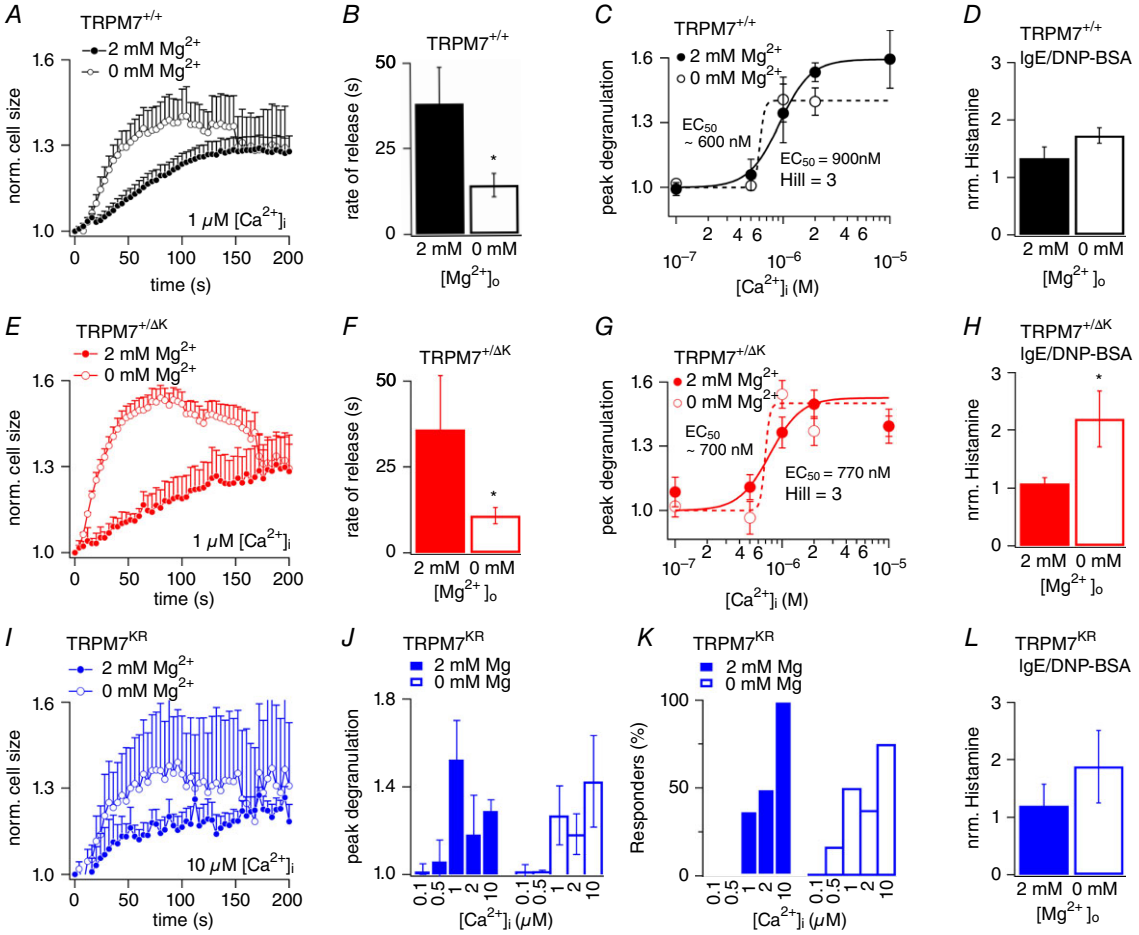

Figure 5. Extracellular Mg^{2+} regulates Ca^{2+}-dependent mast cell degranulation
A, average normalized capacitance measurements of 1 μM $[Ca^{2+}]_i$-induced exocytosis of $TRPM7^{+/+}$ mast cells, in normal external solution containing 2 mM Mg^{2+} (black circles) compared to Mg^{2+}-free (open circles) conditions (n = 5–10). Capacitance as an estimate of cell size (in pF) was measured and plotted as described in Fig. 1. *B*, analysis of the rate of release of the experiment in *A*. Tau was obtained by fitting the data with a capacitance fit function (see Methods). Asterisk indicates $P < 0.02$. *C*, dose response of Ca^{2+}-induced exocytosis of $TRPM7^{+/+}$ mast cells in the presence (2 mM, filled circles) and absence of Mg^{2+} (open circles) (n = 5–10). $[Ca^{2+}]_i$ was clamped as in *A*. The maximal capacitance increase (relative degranulation amplitude) is plotted against $[Ca^{2+}]_i$ and fitted via a dose–response fit function (see Methods; n = 5–10). EC_{50} and Hill coefficients are as indicated in the panel. *E*, average normalized capacitance measurements of 1 μM $[Ca^{2+}]_i$-induced exocytosis of $TRPM7^{+/\Delta K}$ mast cells kept in normal external solution (2 mM Mg^{2+}; red filled circles) compared to Mg^{2+}-free (red open circles) conditions (n = 5–0). Data were acquired and analysed as in *A*. *F*, analysis of the time constant (Tau) of the experiment in *E*. Tau was obtained as in *B*. Asterisk indicates $P < 0.003$. *G*, dose–response curve of $[Ca^{2+}]_i$-induced exocytosis of $TRPM7^{+/\Delta K}$ mast cells in the presence (2 mM, red filled circles) and absence of Mg^{2+} (open circles) (n = 5–9). Note that upon removal of Mg^{2+} the dose–response curves of both $TRPM7^{+/+}$ (black) and $TRPM7^{+/\Delta K}$ (red) derived cells shift to an all-or-none fashion. Data were acquired and analysed as *C*. Error bars indicate SEM. *I*, average normalized capacitance measurements of 10 μM $[Ca^{2+}]_i$-induced exocytosis of $TRPM7^{KR}$ mast cells kept in normal external solution (2 mM Mg^{2+}; blue filled circles) compared to Mg^{2+}-free (open circles) conditions (n = 4 each). Data were acquired and analysed as in *A*. *J*, peak degranulation analysed as in *B* of $TRPM7^{KR}$ mast cells in response to increasing $[Ca^{2+}]_i$ concentrations in the presence (blue filled bars) or absence (open bars) of extracellular Mg^{2+} (n = 4–8). Error bars are SEM. *K*, percentage of $TRPM7^{KR}$ mast cells degranulating in response to $[Ca^{2+}]_i$. *D*, *H* and *L*, histamine release in $TRPM7^{+/+}$, $TRPM7^{+/\Delta K}$ or $TRPM7^{KR}$ mast cells was measured via a HTRF® histamine assay (Cisbio) with or without treatment. Data are presented as mean of three independent experiments and are normalized to the respective untreated controls (spontaneous histamine release). Error bars indicate SEM. IgE-dependent histamine release of $TRPM7^{+/+}$ (black bars) (*D*), $TRPM7^{+/\Delta K}$ (red bars) (*H*) or $TRPM7^{KR}$ mast cells incubated in the presence (open bars) or absence of extracellular Mg^{2+} (filled bars) (*L*). Cells were incubated overnight with 100 ng ml^{-1} IgE anti-DNP antibody and further stimulated with 100 ng ml^{-1} DNP-BSA for 30 min. Note there is no difference in IgE-mediated Ca^{2+}-dependent histamine release between $TRPM7^{+/+}$, $TRPM7^{+/\Delta K}$ and $TRPM7^{KR}$ mast cells; however, the removal of external Mg^{2+} resulted in a significant increase in the histamine secretion of $TRPM7^{+/\Delta K}$ cells ($P < 0.01$).

these experiments with removal of extracellular Mg^{2+} uncovered greatly enhanced mast cell degranulation kinetics in response to 1 μM $[Ca^{2+}]_i$ in TRPM7$^{+/+}$ and TRPM7$^{+/\Delta K}$ (Fig. 5*A* and *E* open circles). The rate analysis using a capacitance fit function (see Methods) of these data showed a significant acceleration of Ca^{2+}-induced degranulation in mast cells from TRPM7$^{+/+}$ and TRPM7$^{+/\Delta K}$ in nominally Mg^{2+} free medium (Fig. 5*A*, *B*, *D* and *E*; TRPM7$^{+/+}$: 2.7 times faster, $P < 0.05$; TRPM7$^{+/\Delta K}$: 3 times faster, $P < 0.002$). Removal of extracellular Mg^{2+} also turned the graded response of degranulation into an all-or-none event in TRPM7$^{+/+}$ and TRPM7$^{+/\Delta K}$, without significantly affecting their respective EC_{50} values (Fig. 5*C* and *F*).

Intracellular Ca^{2+} stimulation was not effective on TRPM7^{KR}, regardless of $[Mg^{2+}]_o$ levels. First, cells responded in an all-or-none fashion, showing no degranulation in response to 100 nM and 500 nM $[Ca^{2+}]_i$ and no clear degranulation pattern between 1 μM and 10 μM $[Ca^{2+}]_i$ (Fig. 5*I* and *J*). Second, the degranulation rate below 10 μM $[Ca^{2+}]_i$ was irregular, ranging from a slow linear increase to a fast exponential release pattern, preventing any meaningful kinetic analysis. Third, not every cell degranulated, even with maximal stimulation at 10 μM $[Ca^{2+}]_i$ (Fig. 5*I* and *K*).

Removal of Mg^{2+} by itself had no effect on basal degranulation as assessed by histamine release using competitive ELISA (data not shown, see Methods). However, under hypomagnesaemic conditions, IgE-DNP-induced histamine release was consistently elevated in all three models, reaching statistical significance for TRPM7$^{+/\Delta K}$ with $P < 0.01$ (Fig. 5*H*). We conclude that the presumed residual kinase activity in the heterozygous TRPM7$^{+/\Delta K}$ mice is sufficient to maintain normal Ca^{2+}-dependent mast cell degranulation. However, in the absence of TRPM7 phosphotransferase activity, Ca^{2+}-dependent degranulation is perturbed. In addition, extracellular Mg^{2+} is involved in regulating the responsiveness of mouse peritoneal mast cells to Ca^{2+}-induced degranulation and IgE-DNP-induced histamine release.

Discussion

Several TRP channels have been implicated in mast cell function so far, including TRPC1, TRPC5, TRPM4 and TRPM7. TRPM4, for instance, has been suggested to play an essential role in mast cell activation and cutaneous anaphylaxis (Freichel *et al.* 2012). Inhibition of the TRPM7 channel via siRNA reduced degranulation and cytokine release in rat bone marrow-derived mast cells (Huang *et al.* 2014). The closely related channel–enzyme TRPM6, however, is not expressed in human (Wykes *et al.* 2007) or murine peritoneal mast cells (Fig. 2*A*), indicating that TRPM6 channel or kinase cannot compensate for the loss of TRPM7. Here, we have shown that diminishing the entire channel–kinase function (TRPM7$^{+/\Delta K}$) or explicitly inactivating the TRPM7 kinase activity (TRPM7^{KR}) changes the intracellular calcium ($[Ca^{2+}]_i$) sensitivity and histamine release in G protein receptor-coupled murine mast cell degranulation independent of channel function. Disrupting normal TRPM7 kinase activity also significantly sensitizes G protein-stimulated histamine release to extracellular Mg^{2+} levels compared to wild-type. Furthermore, an inactive TRPM7 kinase function reduces the response to Ca^{2+}-induced exocytosis (TRPM7^{KR}). However, retaining some TRPM7 kinase activity is sufficient to maintain normal degranulation by Ca^{2+} (TRPM7$^{+/\Delta K}$).

TRPM7 is expressed in synaptic vesicles of sympathetic neurons isolated from rat superior cervical ganglion (SCG) and forms a molecular complex with the synaptic vesicle fusion machinery. A dominant-negative pore mutation of TRPM7 was sufficient to almost completely suppress the amplitude of excitatory postsynaptic potentials (EPSPs), indicating that the channel domain of TRPM7 regulates the synaptic vesicle–plasma membrane fusion and/or the amount of neurotransmitter that is released from a single vesicle (Krapivinsky *et al.* 2006). In mouse peritoneal mast cells, TRPM7 channel activity is strongly suppressed in TRPM7$^{+/\Delta K}$ but not in TRPM7^{KR} (Ryazanova *et al.* 2010) (Fig. 2). Yet, neither $[Ca^{2+}]_i$-induced degranulation rate, nor amplitude, nor IgE-DNP-induced histamine release showed any significant differences between TRPM7$^{+/+}$ and TRPM7$^{+/\Delta K}$ mast cells. In contrast, TRPM7^{KR} mast cells had disrupted degranulation responses despite normal TRPM7 currents (Figs 2 and 5). These results likely exclude involvement of the protein's channel domain in $[Ca^{2+}]_i$-mediated murine mast cell degranulation.

In rat pheochromocytoma (PC12) cells, TRPM7 locates to small synaptic-like vesicles (SSLVs) (Brauchi *et al.* 2008), whose cargo comprises mainly acetylcholine (De Camilli, 1991). It has been shown that TRPM7 co-localizes with the synaptic protein synaptophysin and co-immunoprecipitates with synaptotagmin 1 and synapsin 1 (Krapivinsky *et al.* 2006). Suppression of TRPM7 channel activity using the same dominant-negative pore mutant as in SCG neurons (Krapivinsky *et al.* 2006) strongly suppressed spontaneous as well as stimulated vesicle fusion (Brauchi *et al.* 2008). On the other hand, transfecting a TRPM7 kinase dead mutant into PC12 cells did not alter vesicular fusion frequency, but instead resulted in higher vesicular mobility (Brauchi *et al.* 2008). In mouse peritoneal mast cells isolated from TRPM7$^{+/\Delta K}$ or TRPM7^{KR} mice, G protein-induced degranulation exhibited a much longer delay compared to TRPM7$^{+/+}$ (Fig. 3), which would agree with a concept of decreased granular mobility in this particular cell type. However, TRPM7 channel involvement in G protein-induced mast cell degranulation can be excluded, since

TRPM7 channel activity was completely suppressed in the presence of 100 μM GTPγS (data not shown; Takezawa *et al.* 2004), substance P-induced histamine secretion remained unaffected by the TRPM7 channel inhibitor NS8593 (Fig. 4), and TRPM7$^{+/\Delta K}$ currents in mast cells were strongly suppressed compared to TRPM7^{KR} and wild-type (Fig. 2).

G protein-induced degranulation in mouse mast cells depends on some availability of $[Ca^{2+}]_i$ (Oberhauser *et al.* 1996). Our data show that mouse wild-type mast cells responded steeply to increases in intracellular Ca^{2+} in the presence of a non-hydrolysable GTP analogue. However, mast cells derived from our mouse models with either diminished TRPM7 protein or inactive kinase function (TRPM7$^{+/\Delta K}$ andTRPM7^{KR}, respectively) consistently showed a decreased degranulation rate, a more graded degranulation response with Hill coefficients of 3 rather than 9, and a right-shifted EC_{50} of $[Ca^{2+}]_i$ from 400 nM to 690 nM (Figs 1 and 3). This desensitization mechanism is reflected also in the significantly reduced G protein-coupled receptor-mediated histamine release in mast cells when stimulating with either MIP-1α or substance P (Fig. 4). Thus, it seems that the TRPM7 kinase modulates the efficacy with which Ca^{2+} supports G protein-mediated mast cell degranulation. However, so far, no *in vivo* TRPM7 kinase substrates regulating Ca^{2+} sensitivity or exocytosis have been identified in mast cells.

Contact hypersensitivity (CHS) to the allergen oxazolone is mediated through the high-affinity IgE receptor in murine mast cells (Kobayashi *et al.* 2010). Our previous work identified that the heterologous deletion of the TRPM7 kinase domain (TRPM7$^{+/\Delta K}$) significantly increased oxazolone-induced CHS in these mice (Kobayashi *et al.* 2010). At the same time, TRPM7$^{+/\Delta K}$ mice manifested hypomagnesaemia compared to control. In the current study, we could not detect any difference in IgE-DNP-induced histamine release or Ca^{2+}-induced mast cell degranulation between wild-type and TRPM7$^{+/\Delta K}$ mice (Figs 1 and 5). However, removal of extracellular Mg^{2+} significantly accelerated the rate of mast cell degranulation, turned the Ca^{2+} response into an 'all-or-none event', and slightly increased the histamine release volume, which was significant for TRPM7$^{+/\Delta K}$ (Fig. 5). It is therefore likely that the enhanced CHS phenotype seen in TRPM7$^{+/\Delta K}$ mast cells is due to the systemic hypomagnesaemia seen in this mouse model rather than TRPM7 itself.

In contrast to TRPM7$^{+/\Delta K}$, which might have some residual kinase activity remaining, complete ablation of any phosphotransferase activity in the homozygous TRPM7^{KR} mutant resulted in slight resistance to oxazolone-mediated CHS without any effect on systemic Mg^{2+} status (Ryazanova *et al.* 2014). TRPM7^{KR} mast cells displayed perturbed Ca^{2+}-induced degranulation that did not, however, directly affect IgE-DNP histamine release volume (Fig. 5). This indicates some involvement of the TPRM7 phosphotransferase activity in the Ca^{2+}-induced exocytotic process. It appears, however, that as long as at least some functional TRPM7 kinase activity is maintained (TRPM7$^{+/\Delta K}$), normal Ca^{2+}-induced mast cell degranulation remains protected.

Although the fundamental mechanisms of exocytotic membrane fusion are shared between different cell types, mast cells have evolved their own specialized mechanisms to meet their distinct exocytotic needs. The trafficking of mast cell granules to the cell membrane, for instance, is organized after the activation of a mast cell, unlike in neurons, thus resulting in an extensive reorganization of the cytoskeleton after stimulation, which allows the granules to dock and fuse with the plasma membrane. These dynamic changes are regulated by phosphorylation of myosin IIA, since it is the only myosin isoform present in mast cells (Choi *et al.* 1994). It is likely that the TRPM7 kinase, being able to phosphorylate myosin IIA at various sites (Clark *et al.* 2006), plays a crucial role in this process. Alternatively, the kinase could directly target gene transcription of proteins relevant for exocytosis and release. It was hypothesized that the kinase tags itself via autophosphorylation for cell type-specific nuclear targeting and that a kinase-dead mutant (K1646A) alters the binding of these target molecules (Krapivinsky *et al.* 2014). Thus, impairment of proper kinase function could directly or indirectly affect signalling cascades important for mast cell responses.

Another target candidate for TRPM7 kinase is annexin 1 (Dorovkov & Ryazanov, 2004). In resting mast cells annexin 1 (ANXA1) localizes to the cytoplasmic granules (Oliani *et al.* 2000). Even in degranulated mast cells ANXA1 remains associated with the granule matrix (Oliani & Perretti, 2001). The expression of this protein is increased during the inflammatory response in a model of granulomatous inflammation (Oliani *et al.* 2008). ANXA1 is considered an anti-inflammatory molecule since its expression is upregulated upon glucocorticoid (dexamethasone) treatment (Oliani *et al.* 2000) and compared to control, ANXA1 knock-out mice display higher mast cell degranulation (Damazo *et al.* 2006). Furthermore, phosphorylation of ANXA1 at Ser5 can potentially modulate membrane-binding properties of annexin 1, and thus might regulate insertion of the vesicles into the plasma membrane (Dorovkov & Ryazanov, 2004).

Recently, TRPM7 kinase has been suggested to be cleaved from the channel during apoptosis, thus increasing TRPM7 channel activity, which subsequently is thought to be essential for apoptosis (Desai *et al.* 2012). Further, it has been speculated that TRPM7 kinase affects transcriptional pathways in the heart, via regulation of transcription factors. Its cleavage might allow the kinase to act independently as regulator of transcriptional activity (Sah

et al. 2013). These exciting hypotheses are currently under investigation and highlight the potential biological role of TRPM7 kinase that could also affect mast cell responses.

In summary, we found that the presence of extracellular Mg^{2+} has a stabilizing or protective effect on Ca^{2+}-induced mast cell degranulation independent of TRPM7, providing a cellular link between Mg^{2+} status and systemic inflammatory and allergic responses (Malpuech-Brugere *et al.* 2000). We propose that the TRPM7 kinase activity, but not the channel domain, participates in the regulation of murine mast cell degranulation. A functional TRPM7 kinase assures proper Ca^{2+}-induced exocytosis and regulates the $[Ca^{2+}]_i$ and $[Mg^{2+}]_o$ sensitivity of G protein-coupled receptor-mediated mast cell degranulation by changing granular mobility and/or histamine content. However, *in vivo* TRPM7 kinase substrates regulating exocytosis in mast cells remain to be identified.

References

Aridor M, Rajmilevich G, Beaven MA & Sagi-Eisenberg R (1993). Activation of exocytosis by the heterotrimeric G protein Gi3. *Science* **262**, 1569–1572.

Birnbaumer L & Birnbaumer M (1995). Signal transduction by G proteins: 1994 edition. *J Recept Signal Transduct Res* **15**, 213–252.

Bischoff SC (2007). Role of mast cells in allergic and non-allergic immune responses: comparison of human and murine data. *Nat Rev Immunol* **7**, 93–104.

Brauchi S, Krapivinsky G, Krapivinsky L & Clapham DE (2008). TRPM7 facilitates cholinergic vesicle fusion with the plasma membrane. *Proc Natl Acad Sci USA* **105**, 8304–8308.

Choi OH, Adelstein RS & Beaven MA (1994). Secretion from rat basophilic RBL-2H3 cells is associated with diphosphorylation of myosin light chains by myosin light chain kinase as well as phosphorylation by protein kinase C. *J Biol Chem* **269**, 536–541.

Chubanov V, Mederos y Schnitzler M, Meissner M, Schafer S, Abstiens K, Hofmann T & Gudermann T (2012). Natural and synthetic modulators of SK ($K_{Ca}2$) potassium channels inhibit magnesium-dependent activity of the kinase-coupled cation channel TRPM7. *Br J Pharmacol* **166**, 1357–1376.

Chubanov V, Schlingmann KP, Waring J, Heinzinger J, Kaske S, Waldegger S, Mederos y Schnitzler M & Gudermann T (2007). Hypomagnesemia with secondary hypocalcemia due to a missense mutation in the putative pore-forming region of TRPM6. *J Biol Chem* **282**, 7656–7667.

Claret EJ, Ouled-Diaf J & Seguin P (2003). Homogeneous time resolved fluorescence assay to measure histamine release. *Comb Chem High Throughput Screen* **6**, 789–794.

Clark K, Langeslag M, van Leeuwen B, Ran L, Ryazanov AG, Figdor CG, Moolenaar WH, Jalink K & van Leeuwen FN (2006). TRPM7, a novel regulator of actomyosin contractility and cell adhesion. *EMBO J* **25**, 290–301.

Clark K, Middelbeek J, Dorovkov MV, Figdor CG, Ryazanov AG, Lasonder E & van Leeuwen FN (2008). The α-kinases TRPM6 and TRPM7, but not eEF-2 kinase, phosphorylate the assembly domain of myosin IIA, IIB and IIC. *FEBS Lett* **582**, 2993–2997.

Damazo AS, Yona S, Flower RJ, Perretti M & Oliani SM (2006). Spatial and temporal profiles for anti-inflammatory gene expression in leukocytes during a resolving model of peritonitis. *J Immunol* **176**, 4410–4418.

De Camilli P (1991). Co-secretion of multiple signal molecules from endocrine cells via distinct exocytotic pathways. *Trends Pharmacol Sci* **12**, 446–448.

Deason-Towne F, Perraud AL & Schmitz C (2012). Identification of Ser/Thr phosphorylation sites in the C2-domain of phospholipase C γ2 (PLCγ2) using TRPM7-kinase. *Cell Signal* **24**, 2070–2075.

Desai BN, Krapivinsky G, Navarro B, Krapivinsky L, Carter BC, Febvay S, Delling M, Penumaka A, Ramsey IS, Manasian Y & Clapham DE (2012). Cleavage of TRPM7 releases the kinase domain from the ion channel and regulates its participation in Fas-induced apoptosis. *Dev Cell* **22**, 1149–1162.

Dorovkov MV & Ryazanov AG (2004). Phosphorylation of annexin I by TRPM7 channel-kinase. *J Biol Chem* **279**, 50643–50646.

Freichel M, Almering J & Tsvilovskyy V (2012). The role of TRP proteins in mast cells. *Front Immunol* **3**, 150.

Gilfillan AM & Tkaczyk C (2006). Integrated signalling pathways for mast-cell activation. *Nat Rev Immunol* **6**, 218–230.

Huang L, Ng NM, Chen M, Lin X, Tang T, Cheng H, Yang C & Jiang S (2014). Inhibition of TRPM7 channels reduces degranulation and release of cytokines in rat bone marrow-derived mast cells. *Int J Mol Sci* **15**, 11817–11831.

Johnson JD, Hand WL & King-Thompson NL (1980). The role of divalent cations in interactions between lymphokines and macrophages. *Cell Immunol* **53**, 236–245.

Kaitsuka T, Katagiri C, Beesetty P, Nakamura K, Hourani S, Tomizawa K, Kozak JA & Matsushita M (2014). Inactivation of TRPM7 kinase activity does not impair its channel function in mice. *Sci Rep* **4**, 5718.

Killilea DW & Maier JA (2008). A connection between magnesium deficiency and aging: new insights from cellular studies. *Magnes Res* **21**, 77–82.

Kobayashi M, Nunomura S, Gon Y, Endo D, Kishiro S, Fukunaga M, Kitahata Y, Terui T & Ra C (2010). Abrogation of high-affinity IgE receptor-mediated mast cell activation at the effector phase prevents contact hypersensitivity to oxazolone. *J Invest Dermatol* **130**, 725–731.

Kozak JA, Matsushita M, Nairn AC & Cahalan MD (2005). Charge screening by internal pH and polyvalent cations as a mechanism for activation, inhibition, and rundown of TRPM7/MIC channels. *J Gen Physiol* **126**, 499–514.

Kraeuter SL & Schwartz R (1980). Blood and mast cell histamine levels in magnesium-deficient rats. *J Nutr* **110**, 851–858.

Krapivinsky G, Krapivinsky L, Manasian Y & Clapham DE (2014). The TRPM7 chanzyme is cleaved to release a chromatin-modifying kinase. *Cell* **157**, 1061–1072.

Krapivinsky G, Mochida S, Krapivinsky L, Cibulsky SM & Clapham DE (2006). The TRPM7 ion channel functions in cholinergic synaptic vesicles and affects transmitter release. *Neuron* **52**, 485–496.

Kuehn HS & Gilfillan AM (2007). G protein-coupled receptors and the modification of FcεRI-mediated mast cell activation. *Immunol Lett* **113**, 59–69.

Laffargue M, Calvez R, Finan P, Trifilieff A, Barbier M, Altruda F, Hirsch E & Wymann MP (2002). Phosphoinositide 3-kinase γ is an essential amplifier of mast cell function. *Immunity* **16**, 441–451.

Lorenz D, Wiesner B, Zipper J, Winkler A, Krause E, Beyermann M, Lindau M & Bienert M (1998). Mechanism of peptide-induced mast cell degranulation. Translocation and patch-clamp studies. *J Gen Physiol* **112**, 577–591.

Ma HT & Beaven MA (2009). Regulation of Ca^{2+} signaling with particular focus on mast cells. *Crit Rev Immunol* **29**, 155–186.

Malpuech-Brugere C, Nowacki W, Daveau M, Gueux E, Linard C, Rock E, Lebreton J, Mazur A & Rayssiguier Y (2000). Inflammatory response following acute magnesium deficiency in the rat. *Biochim Biophys Acta* **1501**, 91–98.

Matsushita M, Kozak JA, Shimizu Y, McLachlin DT, Yamaguchi H, Wei FY, Tomizawa K, Matsui H, Chait BT, Cahalan MD & Nairn AC (2005). Channel function is dissociated from the intrinsic kinase activity and autophosphorylation of TRPM7/ChaK1. *J Biol Chem* **280**, 20793–20803.

Mazur A, Maier JA, Rock E, Gueux E, Nowacki W & Rayssiguier Y (2007). Magnesium and the inflammatory response: potential physiopathological implications. *Arch Biochem Biophys* **458**, 48–56.

Miyazaki D, Nakamura T, Toda M, Cheung-Chau KW, Richardson RM & Ono SJ (2005). Macrophage inflammatory protein-1α as a costimulatory signal for mast cell-mediated immediate hypersensitivity reactions. *J Clin Invest* **115**, 434–442.

Nadler MJ, Hermosura MC, Inabe K, Perraud AL, Zhu Q, Stokes AJ, Kurosaki T, Kinet JP, Penner R, Scharenberg AM & Fleig A (2001). LTRPC7 is a Mg.ATP-regulated divalent cation channel required for cell viability. *Nature* **411**, 590–595.

Nakagawa M, Oono H & Nishio A (2001). Enhanced production of IL-1β and IL-6 following endotoxin challenge in rats with dietary magnesium deficiency. *J Vet Med Sci* **63**, 467–469.

Oberhauser AF, Robinson IM & Fernandez JM (1996). Simultaneous capacitance and amperometric measurements of exocytosis: a comparison. *Biophys J* **71**, 1131–1139.

Oliani SM, Christian HC, Manston J, Flower RJ & Perretti M (2000). An immunocytochemical and in situ hybridization analysis of annexin 1 expression in rat mast cells: modulation by inflammation and dexamethasone. *Lab Invest* **80**, 1429–1438.

Oliani SM, Ciocca GA, Pimentel TA, Damazo AS, Gibbs L & Perretti M (2008). Fluctuation of annexin-A1 positive mast cells in chronic granulomatous inflammation. *Inflamm Res* **57**, 450–456.

Oliani SM & Perretti M (2001). Cell localization of the anti-inflammatory protein annexin 1 during experimental inflammatory response. *Ital J Anat Embryol* **106**, 69–77.

Penner R & Neher E (1988). Secretory responses of rat peritoneal mast cells to high intracellular calcium. *FEBS Lett* **226**, 307–313.

Penner R, Pusch M & Neher E (1987). Washout phenomena in dialyzed mast cells allow discrimination of different steps in stimulus-secretion coupling. *Biosci Rep* **7**, 313–321.

Pinxteren JA, O'Sullivan AJ, Larbi KY, Tatham PE & Gomperts BD (2000). Thirty years of stimulus-secretion coupling: from Ca^{2+} to GTP in the regulation of exocytosis. *Biochimie* **82**, 385–393.

Rude RK, Gruber HE, Norton HJ, Wei LY, Frausto A & Kilburn J (2005). Dietary magnesium reduction to 25% of nutrient requirement disrupts bone and mineral metabolism in the rat. *Bone* **37**, 211–219.

Runnels LW, Yue L & Clapham DE (2001). TRP-PLIK, a bifunctional protein with kinase and ion channel activities. *Science* **291**, 1043–1047.

Ryazanova LV, Dorovkov MV, Ansari A & Ryazanov AG (2004). Characterization of the protein kinase activity of TRPM7/ChaK1, a protein kinase fused to the transient receptor potential ion channel. *J Biol Chem* **279**, 3708–3716.

Ryazanova LV, Hu Z, Suzuki S, Chubanov V, Fleig A & Ryazanov AG (2014). Elucidating the role of the TRPM7 alpha-kinase: TRPM7 kinase inactivation leads to magnesium deprivation resistance phenotype in mice. *Sci Rep* **4**, 7599.

Ryazanova LV, Rondon LJ, Zierler S, Hu Z, Galli J, Yamaguchi TP, Mazur A, Fleig A, Ryazanov AG (2010). TRPM7 is essential for Mg^{2+} homeostasis in mammals. *Nat Commun* **1**, 109.

Sagi-Eisenberg R (2007). The mast cell: where endocytosis and regulated exocytosis meet. *Immunol Rev* **217**, 292–303.

Sah R, Mesirca P, Van den Boogert M, Rosen J, Mably J, Mangoni ME & Clapham DE (2013). Ion channel-kinase TRPM7 is required for maintaining cardiac automaticity. *Proc Natl Acad Sci USA* **110**, E3037–E3046.

Schmitz C, Perraud AL, Fleig A & Scharenberg AM (2004). Dual-function ion channel/protein kinases: novel components of vertebrate magnesium regulatory mechanisms. *Pediatr Res* **55**, 734–737.

Schmitz C, Perraud AL, Johnson CO, Inabe K, Smith MK, Penner R, Kurosaki T, Fleig A & Scharenberg AM (2003). Regulation of vertebrate cellular Mg^{2+} homeostasis by TRPM7. *Cell* **114**, 191–200.

Takezawa R, Schmitz C, Demeuse P, Scharenberg AM, Penner R & Fleig A (2004). Receptor-mediated regulation of the TRPM7 channel through its endogenous protein kinase domain. *Proc Natl Acad Sci USA* **101**, 6009–6014.

Weglicki WB, Mak IT, Stafford RE, Dickens BF, Cassidy MM & Phillips TM (1994). Neurogenic peptides and the cardiomyopathy of magnesium-deficiency: effects of substance P-receptor inhibition. *Mol Cell Biochem* **130**, 103–109.

Weglicki WB & Phillips TM (1992). Pathobiology of magnesium deficiency: a cytokine/neurogenic inflammation hypothesis. *Am J Physiol Regul Integr Comp Physiol* **263**, R734–R737.

Weglicki WB, Phillips TM, Freedman AM, Cassidy MM & Dickens BF (1992). Magnesium-deficiency elevates circulating levels of inflammatory cytokines and endothelin. *Mol Cell Biochem* **110**, 169–173.

Wolf FI & Trapani V (2008). Cell (patho)physiology of magnesium. *Clin Sci (Lond)* **114**, 27–35.

Wykes RC, Lee M, Duffy SM, Yang W, Seward EP & Bradding P (2007). Functional transient receptor potential melastatin 7 channels are critical for human mast cell survival. *J Immunol* **179**, 4045–4052.

Yamaguchi H, Matsushita M, Nairn AC & Kuriyan J (2001). Crystal structure of the atypical protein kinase domain of a TRP channel with phosphotransferase activity. *Mol Cell* **7**, 1047–1057.

Additional information

Competing interests

All authors declare no conflict of interest.

Author contributions

S.Z. and A.F. designed the experiments. S.Z., A.S., S.S. and F.Ó.D. performed the experiments and analysed the data. S.Z., A.S., L.V.R., R.P., A.G.R. and A.F. interpreted the data and wrote or revised the manuscript. All authors have approved the final version of the manuscript and agree to be accountable for all aspects of the work. All persons designated as authors qualify for authorship, and all those who qualify for authorship are listed.

Funding

This work was supported by NIH grants P01GM078195 (A.G.R., A.F.) and NIH 5G12 RR003061-22 (University of Hawaii at Manoa Imaging Core), Austrian Science Fund (FWF) grant J2784, Research Executive Agency FP7-PEOPLE-2012-CIG no. 322185 and Deutsche Forschungsgemeinschaft (DFG) TRR-152 (S.Z.). Partial support was provided by a private donation by Mrs Amy Chong (A.F.).

Acknowledgements

We thank L. Tsue, S. Johne, M. K. Monteilh-Zoller, S. Geiger, S. Hunger, S. Hampe and W. Nadolni for excellent technical support.